2006

Rotationally resolved infrared spectrum of the Li+_D2 cation complex

C D. Thompson
University Of Melbourne

C Emmeluth
University Of Melbourne

B L. J Poad
University of Wollongong, bpoad@uow.edu.au

G H. Weddle
University Of Melbourne

E J. Bieske
University Of Melbourne

Rotationally resolved infrared spectrum of the Li+_D2 cation complex

Abstract

The infrared spectrum of mass selected Li +-D 2 cations is recorded in the D-D stretch region (2860-2950 cm -1) in a tandem mass spectrometer by monitoring Li + photofragments. The D-D stretch vibration of Li +-D 2 is shifted by -79 cm -1 from that of the free D 2 molecule indicating that the vibrational excitation of the D 2 subunit strengthens the effective Li +-D 2 intermolecular interaction. Around 100 rovibrational transitions, belonging to parallel K a=0-0, 1-1, and 2-2 subbands, are fitted to a Watson A-reduced Hamiltonian to yield effective molecular parameters. The infrared spectrum shows that the complex consists of a Li + ion attached to a slightly perturbed D 2 molecule with a T-shaped equilibrium configuration and a 2.035 A vibrationally averaged intermolecular separation. Comparisons are made between the spectroscopic data and data obtained from rovibrational calculations using a recent three dimensional Li +-D 2 potential energy surface [R. Martinazzo, G. Tantardini, E. Bodo, and F. Gianturco, J. Chem. Phys. 119, 11241 (2003)].

Keywords

complex, resolved, li, spectrum, infrared, rotationally, _d2, cation

Disciplines

Life Sciences | Physical Sciences and Mathematics | Social and Behavioral Sciences

Publication Details

Thompson, C. D., Emmeluth, C., Poad, B. L. J., Weddle, G. H. & Bieske, E. J. (2006). Rotationally resolved infrared spectrum of the Li+_D2 cation complex. Journal of Chemical Physics, 125 (4), 044310-1-044310-5.

Rotationally resolved infrared spectrum of the Li^+-D_2 cation complex

C. D. Thompson, C. Emmeluth, B. L. J. Poad, G. H. Weddle,[a] and E. J. Bieske[b]
School of Chemistry, University of Melbourne, Melbourne 3010, Australia

(Received 19 May 2006; accepted 5 June 2006; published online 27 July 2006)

The infrared spectrum of mass selected Li^+-D_2 cations is recorded in the D–D stretch region (2860–2950 cm^{-1}) in a tandem mass spectrometer by monitoring Li^+ photofragments. The D–D stretch vibration of Li^+-D_2 is shifted by −79 cm^{-1} from that of the free D_2 molecule indicating that the vibrational excitation of the D_2 subunit strengthens the effective $Li^+\cdots D_2$ intermolecular interaction. Around 100 rovibrational transitions, belonging to parallel K_a=0-0, 1-1, and 2-2 subbands, are fitted to a Watson *A*-reduced Hamiltonian to yield effective molecular parameters. The infrared spectrum shows that the complex consists of a Li^+ ion attached to a slightly perturbed D_2 molecule with a T-shaped equilibrium configuration and a 2.035 Å vibrationally averaged intermolecular separation. Comparisons are made between the spectroscopic data and data obtained from rovibrational calculations using a recent three dimensional Li^+-D_2 potential energy surface [R. Martinazzo, G. Tantardini, E. Bodo, and F. Gianturco, J. Chem. Phys. **119**, 11241 (2003)].
 [DOI: 10.1063/1.2218334]

I. INTRODUCTION

Complexes of alkali metal cations and hydrogen molecules such as Li^+-H_2 are interesting because of their relevance to molecular hydrogen absorption at alkali cation sites in zeolites, their possible participation in astrophysical processes, and their suitability to accurate theoretical treatments. Despite their significance, there are no spectroscopic data on the alkali metal-hydrogen complexes although there have been numerous theoretical studies.

Initial experimental studies of the Li^+-H_2 system were done by Toennies and co-workers who investigated vibrationally and rotationally inelastic collisions between Li^+ and the H_2 and D_2 molecules.[1–4] The first direct observation of Li^+-H_2 was made by Clampitt and Jefferies who found that Li^+ ions solvated by up to six H_2 molecules were ejected when a solid H_2 target was irradiated by a Li^+ beam.[5] Subsequently the binding energy of H_2 to Li^+ was estimated as 6.5±4.6 kcal/mol (2275 cm^{-1}) through appearance potential measurements of Li^+-H_2.[6]

Most theoretical studies of Li^+-H_2 have focused on calculating the equilibrium geometry and vibrational frequencies in the harmonic approximation with the application of increasingly sophisticated levels of *ab initio* theory.[7–31] All existing calculations agree that the Li^+-H_2 complex has a T-shaped C_{2v} equilibrium structure with the Li^+ ion loosely tethered to the H_2 molecule, a binding geometry favored by the electrostatic interaction between the positive charge of the Li^+ and the H_2 quadrupole moment. Several studies have focused on establishing links between the strength of the cation-H_2 interaction and the shift in the H_2 vibrational frequency.[23,31]

A comprehensive understanding of the Li^+-H_2 complex must account for the weak nature of the $Li^+\cdots H_2$ interaction and the large amplitude intermolecular motions which are probably poorly described by the harmonic approximation. The first effort in this direction was by Searles and Von Nagy-Felsobuki who fitted 170 *ab initio* energy points for the Li^+-H_2 with a Padé-approximant function with a Dunham expansion variable.[20] Subsequently, Røeggen *et al.* calculated a $Li^+\cdots H_2$ interaction potential for fixed H_2 bond length that was used in scattering calculations to model the mobility of Li^+ ions in H_2 gas.[29] More recently, Bulychev *et al.* calculated a three-dimensional (3D) potential energy surface (PES) at the MP2 level and used it to determine variationally the energies for the J=0 vibrational states of Li^+-H_2, Li^+-D_2, and Li^+-T_2.[30]

In a comprehensive theoretical study of the Li^+-H_2 system, Martinazzo, Tantardini, Bodo, and Gianturco (MTBG) calculated a three-dimensional potential energy surface primarily to understand the astrophysically important $LiH^+ + H \rightarrow Li^+ + H_2$ and $LiH + H^+ \rightarrow Li + H_2^+$ reactions.[32] The energy points, determined with complete active self-consistent field reference functions and a large Li basis set, were fitted to a functional form that accounts for the important long-range contributions to the interactions. The MTBG surface possesses a shallow well in a T-shaped C_{2v} geometry with a $Li^+\cdots H_2$ separation of 1.92 Å and a depth of 0.286 eV (2309 cm^{-1}) with respect to the Li^+-H_2 asymptote. As shown in Fig. 1 there is an appreciable 1680 cm^{-1} barrier to H_2 internal rotation in the linear configuration. The MTBG PES was subsequently used in variational calculations to determine the J=0 rovibrational states of the Li^+-H_2 complex.[33]

In this work we report an infrared photodissociation spectrum of Li^+-D_2 in the D–D stretch region. The spectrum, which features full rotational resolution, provides critical information to test and refine potential energy surface for the $Li^+\cdots H_2$ interaction.

[a]Also at Department of Chemistry, Fairfield University, Fairfield, Connecticut.
[b]Electronic mail: evanjb@unimelb.edu.au

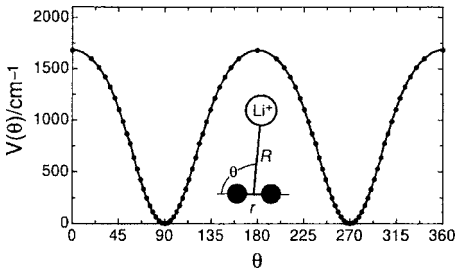

FIG. 1. Angular potential energy curve for the $Li^+\cdots D_2$ interaction at fixed D–D separation (r=0.750 Å). The energies at each angle correspond to the minimum of the MTBG PES along the intermolecular stretch coordinate (R) (Ref. 32).

II. EXPERIMENTAL METHODS

The infrared spectrum of $^7Li^+-D_2$ was measured by scanning the IR wavelength over the D–D stretch region while monitoring production of Li^+ photofragments. Vibrational energy originally localized in the D–D stretch coordinate, migrates into the weak intermolecular bond, leading to its rupture and the liberation of Li^+ photofragments.

The Li^+-D_2 complexes were generated in a supersonic expansion of D_2 (stagnation pressure of 6 bars) passing over a rotating metal alloy rod (10% Li/90% Al). The rotating rod was irradiated with the fundamental (1064 nm, 7 mJ/pulse), doubled (532 nm, 3 mJ/pulse), and quadrupled (266 nm, 1 mJ/pulse) output of a pulsed Nd:YAG (yttrium aluminum garnet) laser (20 Hz repetition rate).

The tandem mass spectrometer apparatus, which has been described previously,[34] comprises a primary quadrupole mass filter for the selection of the parent $^7Li^+-D_2$ ions, an octopole ion guide, where the ions are overlapped with the counterpropagating output of a pulsed, tuneable IR radiation source [Continuum Mirage 3000 optical parametric oscillator (OPO) 0.017 cm^{-1} bandwidth], and a second quadrupole mass filter tuned to the mass of Li^+ fragment ions. Photofragments were sensed with a microchannel plate coupled to a scintillator and photomultiplier tube.

Wavelength calibration was accomplished using a wavemeter (HighFinesse WS/7) to measure the wavelength of the signal output from the first stage of the optical parametric oscillator and the 532 nm output of the seeded Nd:YAG laser. The transition wave numbers were corrected to account for the Doppler shift resulting from the ions' 10 eV translational energy in the octopole ion guide. The absolute uncertainty of the line wave numbers is decided by the uncertainty of the ions' energy in the octopole ion guide and is estimated as 0.10 cm^{-1}. The relative uncertainties of the lines' wave numbers are estimated as 0.015 cm^{-1}. The lines' intensities are not normalized for laser power or parent ion signal intensity which exhibits considerable shot-to-shot and longer term fluctuations.

III. RESULTS AND DISCUSSION

A. Infrared spectrum of Li^+-D_2

The Li^+-D_2 complex is expected to have a T-shaped equilibrium geometry favored by the electrostatic interaction between the Li^+ cation and the quadrupole moment of the D_2 molecule (see Fig. 1). The minimum energy geometry on the MTBG potential energy surface is a T-shaped structure with D–D separation of 0.751 Å and intermolecular separation of 1.916 Å. This structure corresponds to rotational constants A=29.7 cm^{-1}, B=1.79 cm^{-1}, and C=1.69 cm^{-1} and asymmetry parameter κ=−0.993. Because the barrier to internal rotation of the D_2 subunit (1680 cm^{-1}) is much larger than the D_2 rotational constant ($b_{DD}\sim$30 cm^{-1}), the internal rotation is largely quenched and the system should approach the near prolate asymmetric top limit. Therefore, the quantum number associated with the projection of the total angular momentum onto the intermolecular axis (K_a) is nearly good. Even and odd K_a states correspond, respectively, to Li^+ attached to the *ortho* and *para* modifications of D_2. For normal D_2 gas the *ortho* (even j) and *para* (odd j) forms occur in 2:1 ratio. Direct collisional relaxation between the two forms should be extremely inefficient in the supersonic expansion, although the exchange of D_2 ligands attached to the Li^+ is probably a facile process. Because the transition moment for excitation of the D–D stretch lies along the intermolecular bond (i.e., a parallel transition), the IR spectrum should consist of overlapping K_a=0-0, 1-1, 2-2, etc., subbands.

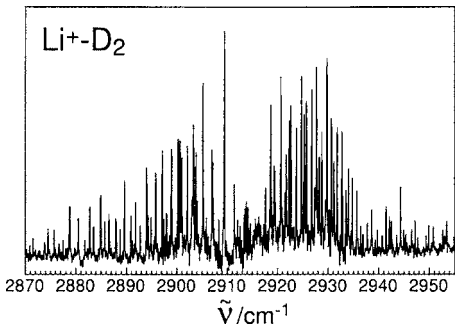

FIG. 2. Infrared spectrum of $^7Li^+-D_2$ in the D–D stretch region obtained by monitoring the $^7Li^+$ photofragment signal as the IR wavelength was scanned. An expanded view of the central part of the spectrum is shown in Fig. 3.

As expected from the considerations outlined above, the experimental Li^+-D_2 spectrum shown in Fig. 2 has the appearance of a parallel transition of a near prolate asymmetric rotor with K_a=0-0, K_a=1-1, and K_a=2-2 subbands. An expanded view of the central part of the spectrum is shown in Fig. 3 where the Q branches of the K_a=1-1, K_a=2-2, and K_a=3-3 subbands are clearly apparent. The K_a=1-1 Q

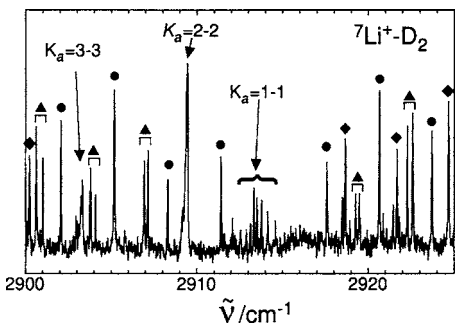

FIG. 3. Central part of the $^7Li^+-D_2$ IR spectrum. The K_a=0-0 transitions are marked by filled circles (●), the K_a=1-1 transitions by triangles (▲), and K_a=2-2 transitions by diamonds (♦).

TABLE I. Constants in cm^{-1} for Li^+-D_2 obtained by fitting the D–D stretch band transitions to a Watson *A*-reduced Hamiltonian. Errors in the last significant figure are given in brackets.

	$K_a=0$	$K_a=1$	$K_a=2$	$K_a=0,1,2$
B''		1.5960(8)		1.5986(6)
C''		1.4971(9)		1.5000(6)
$\bar{B}''$	1.5496(6)	1.5466(9)	1.5406(30)	1.5493(6)
$D_J''\times10^4$	1.271(20)	1.119(55)	1.17(16)	1.163(17)
$D_{JK}''\times10^3$				−2.27(16)
B'		1.5913(7)		1.5935(6)
C'		1.4909(8)		1.4935(6)
$\bar{B}'$	1.5438(5)	1.5411(8)	1.5358(23)	1.5435(6)
$D_J'\times10^4$	1.246(16)	1.111(40)	1.15(10)	1.125(14)
$D_{JK}'\times10^3$				2.10(14)
ΔA[a]				−1.258(3)
ν_0[b]	2914.623(7)	2913.359(6)	2909.586(14)	2914.620(5)
rms$\times10^3$	6.0	7.7	4.1	8.5

[a]$\Delta A=A'-A''$. The value of A'' was fixed to 29.907 cm^{-1}
[b]Subband origins are given for $K_a=0$, $K_a=1$, and $K_a=2$ subbands.

branch exhibits several resolved transitions, whereas the $K_a=2$-2 and $K_a=3$-3 *Q* branches appear as single peaks with maxima at 2909.58 and 2903.45 cm^{-1}, respectively. Also obvious is the band gap between the *P* and *R* branches of the $K_a=0$-0 subband and the asymmetry doubling in the *P* and *R* branch transitions of the $K_a=1$-1 subband. The asymmetry doubling is not resolved for the $K_a=2$-2 subband. Altogether, 30 lines were identified for the $K_a=0$-0 subband, 45 lines in the *P* and *R* branches and 7 lines in the *Q* branch of the $K_a=1$-1 subband, and 14 lines in the *P* and *R* branches of the $K_a=2$-2 subband. The transitions' wave numbers along with assignments in terms of a semirigid asymmetric rotor model (Sec. III B) are available as supplementary material.[35]

B. Asymmetric rotor analysis

The transition wave numbers for the $K_a=0$-0, 1-1, and 2-2 subband lines were fitted to an *A*-reduced Watson Hamiltonian, including D_J and D_{JK} distortion terms. The value of A'' was fixed to 29.907 cm^{-1}, corresponding to the *B* rotational constant of the free D_2 molecule.[36] The fit of the parallel transition determines $\Delta A=A'-A''$ but is relatively insensitive to A' and A'' themselves. Each of the $K_a=0$-0, 1-1, and 2-2 subbands was also fitted separately. Resulting parameters are listed in Table I. Differences between experimental transition frequencies and those calculated using the fitted parameters are included with the supplementary material.[35]

Generally, the spectroscopic constants are compatible with expectations based on previous *ab initio* calculations. For example, the ground and excited state vibrationally averaged $Li^+\cdots H_2$ separations estimated from $\bar{B}''$ and $\bar{B}'$ are 2.035 and 2.038 Å, respectively, which are comparable with equilibrium separations determined in *ab initio* calculations. For example, recent MP2/aug-cc-pVQZ calculations give an equilibrium $Li^+\cdots H_2$ intermolecular separation of 2.01 Å.[31]

Consideration of the spectroscopic data in Table I suggests that even in the ground vibrational state Li^+-D_2 undergoes large amplitude vibrational excursions, particularly in the bending/hindered internal rotation coordinate. For a rigid planar molecule the inertial defect $\Delta=1/C-1/B-1/A$ should be zero. Taking the experimental values for B'' and C'' (Table I) one finds $A''=24.3$ cm^{-1}, corresponding to a vibrationally averaged D–D separation of 0.83 Å. This represents a large increase (by 0.08 Å) in the D–D bond length from the free D_2 molecule value ($\langle\langle r\rangle\rangle=0.75$ Å), which is unlikely to be caused by the relatively weak interaction with the Li^+ ion. Indeed, the equilbrium D–D separation on the MTBG surface is 0.751 Å. The alternative to a large distortion of the D_2 subunit is that the effective molecular parameters are influenced by the large amplitude bending/hindered rotation of the D_2 subunit. As pointed out by Nesbitt and co-workers,[37,38] the unquenched hindered internal rotation tends to exaggerate the asymmetry doubling and consequently $B-C$, leading to a nonzero inertial defect. The effect increases as the hindering barrier decreases.

TABLE II. Energies (in cm^{-1}) for the lowest $J=0-4$ levels of Li^+-D_2 calculated using the MTBG PES (Ref. 32) Even and odd K_a levels correspond to Li^+ interacting with *ortho* and *para* D_2, respectively. At bottom are rotational constants obtained by independently fitting the $K_a=0-3$ manifolds' levels to a second order polynomial in $J(J+1)$.

J	$K_a=0$	$K_a=1$	$K_a=2$	$K_a=3$
0	0			
1		32.762		
	3.257	32.872		
2		39.3154	127.656	
	9.768	39.485	127.656	
3		48.737	137.367	283.582
	19.527	49.398	137.369	283.582
4		61.502	150.304	296.440
	32.525	62.602	150.307	296.440
$\bar{B}$	1.6287	1.6266	1.6205	1.6073
$D_J\times10^4$	1.22	1.12	1.04	

C. Comparison with calculated energy levels

Rovibrational calculations were undertaken using the MTBG surface to derive further insights into the Li^+-D_2 system. Energies of the lower rovibrational levels of $^7Li^+-D_2$ were calculated variationally employing the TRIATOM program[39] with a basis set comprising 20 Morse functions in the D–D stretch, 18 Morse functions in the intermolecular stretch, and 14 Legendre functions for the angular coordinate. The masses of the Li and D atoms were taken to be 7.016 and 2.014 amu, respectively.

Energies for the lower $J=0-4$ rovibrational levels, converged to $<10^{-3}$ cm^{-1}, are listed in Table II. To facilitate comparisons with the experimental data, energies for the $K_a=0$, 1, and 2 manifolds were fitted independently to a polynomial in $J(J+1)$. Results from these fits are also given in Table II. Even and odd K_a levels correspond to Li^+ interacting with *ortho* and *para* D_2, respectively. The ground ($v_{DD}=0$, $v_s=0$, $v_b=0$, $J=0$) state of Li^+-D_2 lies 1858 cm^{-1} below the $Li^++D_2(v_{DD}=0,j=0)$ asymptote. Due to its lower

TABLE III. Data relating to asymmetry splittings in the $K_a=1$ manifolds (units are cm^{-1}).

J	$\Delta''(J)_{calc}$	$\bar{\Delta}(J)_{expt}$ [a]	$\Delta_1''(J)_{calc}$ [b]	$\Delta_1''(J)_{expt}$ [b]	$\Delta_1'(J)_{expt}$ [c]
1	0.110	0.098	0.441	0.400	0.410
2	0.331	0.307	0.992	0.923	0.916
3	0.661	0.613	1.761		
4	1.100				

[a] $\bar{\Delta}(J)=\frac{1}{2}(\Delta''(J)+\Delta'(J))$.
[b] $\Delta_1''(J)=\Delta''(J)+\Delta''(J+1)$.
[c] $\Delta_1'(J)=\Delta'(J)+\Delta'(J+1)$.

zero point energy Li^+-D_2 is 126 cm^{-1} more strongly bound than the Li^+-H_2 isotopomer ($D_0=1732$ cm^{-1}; Ref. 33).

The experimental $\bar{B}''$ value is around 5% less than the corresponding calculated value (Tables I and II), implying that the MTBG surface slightly underestimates the vibrationally averaged $Li^+\cdots D_2$ bond length. The vibrationally averaged separation ($\langle\langle R\rangle\rangle$) estimated from the experimental $\bar{B}''$ value (2.035 Å) is 0.056 Å longer than the value determined from the $\bar{B}$ found from the rovibrational calculations (1.979 Å). In contrast, the vibrationally averaged intermolecular separation calculated by Bulychev *et al.* ($\langle\langle R\rangle\rangle$ =2.051 Å) is closer to the experimental value, overestimating it by 0.016 Å.[30]

As mentioned in Sec. III B the asymmetry splittings are sensitive to details of the $Li^+\cdots D_2$ PES, increasing as the hindering barrier for D_2 internal rotation decreases and also as the intermolecular bond length shortens. For this reason it would be interesting to compare experimental and calculated $K_a=1$ asymmetry splittings. Unfortunately, it is impossible to determine the lower and upper state splittings [$\Delta''(J)$ and $\Delta'(J)$] directly from the infrared spectrum. However, from combination differences one can ascertain $\Delta_1''(J)=\Delta''(J)+\Delta''(J+1)$, $\Delta_1'(J)=\Delta'(J)+\Delta'(J+1)$, and $\bar{\Delta}(J)=\frac{1}{2}(\Delta''(J)+\Delta'(J))$. The experimental and calculated data are compiled in Table III. Firstly, it is interesting to note that the experimental $\Delta_1''(J)$ and $\Delta_1'(J)$ values are very similar, confirming that the vibrational excitation of the D_2 subunit has little effect on the molecular geometry or the effective tunneling barrier. Comparisons of $\Delta_1''(J)_{calc}$ and $\Delta_1''(J)_{expt}$, indicate that the calculated splittings slightly exceed the experimental splittings. At this stage it is uncertain whether the primary cause for the discrepancy is the MTBG surface's underestimation of the $Li^+\cdots D_2$ intermolecular separation or underestimation of the effective tunneling barrier.

D. Intermolecular modes

Rovibrational calculations using the MTBG surface give frequencies of $\nu_s=365$ cm^{-1} for the intermolecular stretch and $\nu_b=503$ cm^{-1} for the intermolecular bend. Corresponding values calculated by Bulychev *et al.* are $\nu_s=329.8$ cm^{-1} and $\nu_b=447.2$ cm^{-1}.[30] The calculated intermolecular stretch frequencies correspond reasonably well to rough estimates for the harmonic frequencies made using the $\bar{B}$ and D_J values ($\omega_s''=347$ cm^{-1} and $\omega_s'=351$ cm^{-1}). In future it may be possible to measure the $\nu_{DD}+\nu_s$ and $\nu_{DD}+\nu_b$ combination bands providing direct information on the intermolecular modes.

E. Ground/excited state changes and vibrational redshift

The IR spectrum provides information on the dependence of the $Li^+\cdots D_2$ intermolecular interaction on the vibrational state of the D_2 molecule. Because the high frequency D–D stretch vibration is effectively adiabatically decoupled from the lower frequency intermolecular stretching and bending motions, one can consider the ground and excited states of the system as consisting of a Li^+ ion interacting with a D_2 molecule in the $v_{DD}=0$ and $v_{DD}=1$ states. From this perspective the effective $Li^+\cdots D_2(v_{DD}=1)$ potential surface is deeper than the $Li^+\cdots D_2(v_{DD}=0)$ potential surface by around 79.0 cm^{-1} [the redshift of the $v_{DD}=1\leftarrow v_{DD}=0$ transition of Li^+-D_2 from the $Q_1(0)$ transition of the free D_2 molecule at 2993.6 cm^{-1}; Ref. 36].

The observed redshift is close to the shifts calculated by Bulychev *et al.* (77.1 cm^{-1}) in their 3D anharmonic vibrational calculations[30] and by Bishop and Cybulski (80.1 cm^{-1}), who estimated the frequency shift by solving the one-dimensional Schrödinger equation for the D_2 molecule perturbed by the attached Li^+.[23]

The redshift and enhancement of the intermolecular bond strength, which have been observed in other ion complexes containing H_2 and D_2, including H_2-HCO^+ (Ref. 40) and Cl^--H_2,[41] can be seen as resulting from increases in the vibrationally averaged quadrupole moment and polarizability of D_2 of 5%–8% going from $v_{DD}=0$ to $v_{DD}=1$, enhancing the charge-quadrupole electrostatic and charge-induced-dipole induction intermolecular interactions.

Surprisingly the A, B, and C rotational constants obtained from the semirigid rotor analysis decrease when the D_2 subunit is vibrationally excited, demonstrating that, notwithstanding the 79 cm^{-1} increase in the effective interaction energy, there is a slight increase in the vibrationally averaged intermolecular separation. The decrease in A is expected since the rotational constant of the free D_2 molecule decreases by 1.06 cm^{-1} going from $v_{DD}=0$ to $v_{DD}=1$.[36] Decreases in the B and C constants are more surprising. We note that Bulychev *et al.* predicted a similar effect, finding that the vibrationally averaged intermolecular separation increased by 0.004 Å when the D–D stretch is excited.[30] The form of the MTBG surface is also consistent with the vibrationally induced increase in the intermolecular separation. As can be seen in Fig. 4 where the equilibrium $Li^+\cdots D_2$ intermolecular separation is plotted as a function of the D–D separation, there is a highly nonlinear dependence of the equilibrium intermolecular bond length on the D–D bond separation so that averaging over the D–D vibrational stretch wave function will lead to a larger mean intermolecular separation for the $v_{DD}=1$ state than for the $v_{DD}=0$ state.

F. Vibrational predissociation dynamics of Li^+-D_2

The observed transitions access quasibound levels that are coupled to the $Li^++D_2(v_{DD}=0)$ continuum. Widths of the individual rovibrational lines provide information on the vibrational predissociation rate. It is easiest to estimate the widths of the $K_a=0$-0 lines since they are the most intense. Fitting the lines with a Voigt profile with the full width at

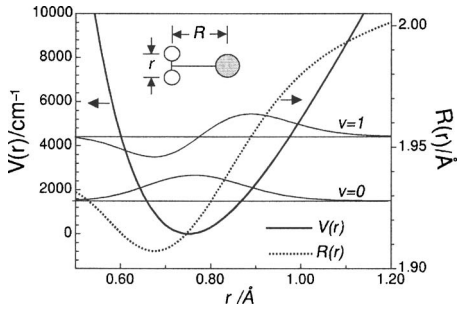

FIG. 4. Plots of potential energy vs D–D separation (solid line) and the equilibrium $Li^+\cdots D_2$ intermolecular separation vs D–D separation (dotted line) for the MTBG PES (Ref. 32). Also shown are the two lowest one-dimensional D–D stretch energy levels and associated wave functions. Note the highly nonlinear dependence of the intermolecular separation on the D–D separation.

half maximum of the Gaussian component fixed to 0.017 cm^{-1} (the bandwidth of the OPO IR radiation) gives a Lorentzian component of $(3.5\pm0.7)\times10^{-2}$ cm^{-1} that is apparently independent of J'. The linewidth corresponds to an upper state lifetime of $\tau_{vp}=150$ ps. We caution that this value for τ_{vp} should be taken as a lower limit for the lifetime as the lines may be power broadened or Doppler broadened due to the ions having a spread of energy in the octopole region where they overlap with IR radiation. It should be remarked that using the same IR light source and tandem mass spectrometer (albeit with a different ion source) we have observed narrower, laser-limited transitions for the $Br^-–D_2$ and $I^-–D_2$ anion complexes.[42,43] Nevertheless, it is interesting to note that Sanz *et al.* have calculated lifetimes in the 100–400 ps range for quasibound $v_{HH}=1$ levels of $Li^+–H_2$.[33]

IV. CONCLUSIONS

The main conclusions of this work can be summarized as follows:

(1) The $Li^+–D_2$ complex possesses a rotationally resolved D–D stretch band redshifted by 79 cm^{-1} from the fundamental of the D_2 diatomic molecule.
(2) The $Li^+–D_2$ complex has a T-shaped equilibrium structure with an average intermolecular $Li^+\cdots D_2$ separation of 2.035 Å, increasing by 0.003 Å when the D_2 subunit is vibrationally excited.
(3) From rovibrational line broadening a lower limit for the predissociation lifetime for $Li^+–D_2(\nu_{DD}=1)$ is 150 ps.

ACKNOWLEDGMENTS

The authors are grateful to the Australian Research Council and the University of Melbourne for supporting this research. This work was supported by a fellowship within the Postdoc-Programme of the German Academic Exchange Service (DAAD). The authors are most grateful to Professor Gianturco and Professor Tantardini for supplying the MTBG $Li^+–H_2$ PES.

[1] J. Schottle and J. Toennies, Z. Phys. **214**, 472 (1968).
[2] R. David, M. Faubel, and J. Toennies, Chem. Phys. Lett. **18**, 87 (1973).
[3] G. Barg and J. Toennies, Chem. Phys. Lett. **51**, 23 (1977).
[4] G. Barg, G. Kendall, and J. Toennies, Chem. Phys. **16**, 243 (1976).
[5] R. Clampitt and D. K. Jefferies, Nature (London) **226**, 141 (1970).
[6] C. H. Wu, J. Chem. Phys. **71**, 783 (1979).
[7] A. A. Wu and F. O. Ellison, J. Chem. Phys. **47**, 1458 (1967).
[8] R. D. Poshusta, J. A. Haugen, and D. F. Zetik, J. Chem. Phys. **51**, 3343 (1969).
[9] J. Easterfield and J. W. Linnett, Nature (London) **226**, 142 (1970).
[10] R. C. Raffenetti and K. Ruedenberg, J. Chem. Phys. **59**, 5978 (1971).
[11] W. Kutzelnigg, V. Staemmler, and L. Hoheisel, Chem. Phys. **1**, 27 (1973).
[12] J. D. Switalski, J. T. J. Huang, and M. E. Schwartz, J. Chem. Phys. **60**, 2252 (1974).
[13] N. K. Ray and J. Switalski, Theor. Chim. Acta **41**, 329 (1976).
[14] N. K. Ray and S. P. Mehandru, Pramana **10**, 201 (1978).
[15] A. S. Zyubin, A. A. Gorbik, and O. P. Charkin, Zh. Strukt. Khim. **26**, 31 (1985).
[16] B. H. Cardelino, W. H. Eberhardt, and R. F. Borkman, J. Chem. Phys. **84**, 3230 (1986).
[17] D. A. Dixon, J. L. Gole, and A. Komornicki, J. Phys. Chem. **92**, 2134 (1988).
[18] D. A. Dixon, J. L. Gole, and A. Komornicki, J. Phys. Chem. **92**, 1378 (1988).
[19] L. A. Curtiss and J. A. Pople, J. Phys. Chem. **92**, 894 (1988).
[20] D. J. Searles and E. I. Von Nagy-Felsobuki, Phys. Rev. A **43**, 3365 (1991).
[21] B. K. Rao and P. Jena, Europhys. Lett. **20**, 307 (1992).
[22] I. Tamassy-Lentei and J. Szaniszlo, Acta Phys. Hung. **74**, 399 (1994).
[23] D. M. Bishop and S. M. Cybulski, Chem. Phys. Lett. **230**, 177 (1994).
[24] B. S. Jursic, THEOCHEM **491**, 11 (1999).
[25] R. Davy, E. Skoumbourdis, and T. Kompanchenko, Mol. Phys. **97**, 1263 (1999).
[26] E. Bodo, F. A. Gianturco, R. Martinazzo, A. Forni, M. Famulari, and A. Raimondi, J. Phys. Chem. A **104**, 11972 (2000).
[27] I. Tamassy-Lentei and J. Szaniszlo, THEOCHEM **501–502**, 403 (2000).
[28] M. Barbatti, G. Jalbert, and M. A. C. Nascimento, J. Chem. Phys. **114**, 2213 (2001).
[29] I. Røeggen, H. Skullerud, T. Løvaas, and D. K. Dysthe, J. Phys. B **35**, 1707 (2002).
[30] V. P. Bulychev, K. M. Bulanin, and M. O. Bulanin, Opt. Spectrosc. **96**, 205 (2004).
[31] J. G. Vitillo, A. Damin, A. Zecchina, and G. Ricchiardi, J. Chem. Phys. **122**, 114311/1 (2005).
[32] R. Martinazzo, G. Tantardini, E. Bodo, and F. Gianturco, J. Chem. Phys. **119**, 11241 (2003).
[33] C. Sanz, E. Bodo, and F. A. Gianturco, Chem. Phys. **314**, 135 (2005).
[34] D. A. Wild and E. J. Bieske, Int. Rev. Phys. Chem. **22**, 129 (2003).
[35] See EPAPS Document No. E-JCPSA6-125-012627 for a table listing the measured transition wavenumbers for the D–D stretch band of $Li^+\cdots D_2$. Given in brackets are the differences (last 2 significant figures) between the experimental values and values calculated using an A-reduced Watson Hamiltonian and the parameters in Table I of the paper. This document can be reached via a direct link in the online article's HTML reference section or via the EPAPS homepage (http://www.alp.org/pubservs/epaps.html).
[36] K. P. Huber and G. Herzberg, *Molecular Spectra and Molecular Structure IV. Constants of Diatomic Molecules* (Van Nostrand Reinhold, New York, 1979).
[37] D. J. Nesbitt and R. Naaman, J. Chem. Phys. **91**, 3801 (1989).
[38] C. Lovejoy, D. Nelson, and D. J. Nesbitt, J. Chem. Phys. **87**, 5621 (1987).
[39] J. Tennyson, Comput. Phys. Rep. **4**, 1 (1986).
[40] E. J. Bieske, S. A. Nizkorodov, F. R. Bennett, and J. P. Maier, J. Chem. Phys. **102**, 5152 (1995).
[41] D. A. Wild, R. L. Wilson, P. S. Weiser, and E. J. Bieske, J. Chem. Phys. **113**, 10154 (2000).
[42] D. A. Wild, P. S. Weiser, and E. J. Bieske, J. Chem. Phys. **115**, 6394 (2001).
[43] D. A. Wild and E. J. Bieske, J. Chem. Phys. **121**, 12276 (2004).